Isolated sub-30-attosecond pulse generation using a multicycle two-color chirped laser and a static electric field*

Zhang Gang-Tai(张刚台)†

Department of Physics and Information Technology, Baoji University of Arts and Sciences, Baoji 721016, *China*

(Received 9 September 2013; revised manuscript received 7 October 2013; published online 10 February 2014)

We present a theoretical investigation of high-order harmonic generation in a chirped two-color laser field, which is synthesized by a 10-fs/800-nm fundamental chirped pulse and a 10-fs/1760-nm subharmonic pulse. It is shown that a supercontinuum can be produced using the multicycle two-color chirped field. However, the supercontinuum reveals a strong modulation structure, which is not good for the generation of an isolated attosecond pulse. By adding a static electric field to the multicycle two-color chirped field, not only the harmonic cutoff is extended remarkably, but also the quantum paths of the high-order harmonic generation (HHG) are modified significantly. As a result, both the extension of the supercontinuum and the selection of a single quantum path are achieved, producing an isolated 23-as pulse with a bandwidth of about 170.6 eV. Furthermore, the influences of the laser intensities on the supercontinuum and isolated attosecond pulse generation are investigated.

Keywords: high-order harmonic, attosecond pulse generation, supercontinuum, combined field

PACS: 32.80.Rm, 42.65.Ky, 42.65.Re **DOI:** 10.1088/1674-1056/23/4/043202

1. Introduction

When an intense laser interacts with atoms and molecules, high-order harmonics can be generated as a consequence of highly nonlinear dynamics.[1–3] Generally speaking, a typical spectrum of high-order harmonic generation (HHG) shows a rapid decrease for the first few harmonics, followed by a broad plateau of almost constant conversion efficiency, ending up with a sharp cutoff. Because HHG covers a broad spectral width from infrared to the soft X-ray region with equidistant frequency, it has become a candidate for breaking through the femtosecond limit. Additionally, HHG is a unique way to produce an isolated attosecond pulse experimentally. Currently, the most well-known theory to describe the HHG is the semiclassic three-step model.[4] According to this model, the electron first tunnels through the barrier formed by the Coulomb potential and the laser field. Then, it oscillates and accelerates in the laser field. Finally, it can recombine with the parent ion emitting a photon with the maximum energy given by $E_{\text{cut off}} = I_{\text{p}} + 3.17U_{\text{p}}$, where I_{p} and U_{p} are the atomic ionization potential and the ponderomotive energy of the electron, respectively. This process occurs every half-cycle and leads to an attosecond-pulse train. Since practical application prefers an isolated pulse, a series of methods have been explored to extract single attosecond pulses. The first method is to utilize few-cycle driving pulses.[5,6] Using this straightforward method, an isolated 80-as pulse has been realized by a 3.3-fs/720-nm carrier-envelope phase (CEP) stabilized laser field.[7] The second method is a polarization gating technique.[8,9] Using this approach, a single 130-as XUV pulse has been demonstrated experimentally.[9] Moreover, the double optical gating (DOG)[10–12] and generalized DOG (GDOG)[13] have been proposed for producing isolated attosecond pulses. Very recently, Zhao *et al.*[14] reported on the generation of an isolated 67-as pulse, which is the shortest attosecond pulse to the best of our knowledge, from an extreme UV supercontinuum covering 55 eV∼130 eV generated by the double optical gating technique. With these techniques mentioned above, scientists can generate a single attosecond pulse. However, the durations of isolated attosecond pulses are still significantly longer than the time scale of electron motion in atoms, i.e., 24 as. It has been suggested that the bandwidth of the attosecond pulse is more important than the duration in attosecond science.[15] Therefore, there is an urgent need to generate isolated attosecond pulses with broader bandwidth and shorter pulse duration.

Presently, there is great interest in the generation of isolated attosecond pulses with a driving pulse with a longer duration, which can avoid the stringent requirement for an available ultrafast laser source (sub-5 fs) in the single laser field. It has been proposed that a two-color control scheme can effectively generate an isolated attosecond pulse in the multicycle regime.[16–18] With this controlling scheme, some authors have successfully synthesized a broadband isolated attosecond pulse.[19–24] Luo *et al.*[19] showed that the harmonic cutoff and the supercontinuum width can be dramatically extended, which can support the generation of an isolated sub-100-as pulse with a tunable central wavelength. Chen *et al.*[20]

*Project supported by the Science Foundation of Baoji University of Arts and Sciences, China (Grant No. ZK11061) and the Natural Science Foundation of Education Committee of Shaanxi Province, China (Grant No. 2013JK0637).

†Corresponding author. E-mail: gtzhang79@163.com

© 2014 Chinese Physical Society and IOP Publishing Ltd

showed that an intense isolated 39-as pulse can be obtained by using an intense multi-cycle 800-nm laser in combination with its 27th harmonic pulse. Zeng *et al.*[21] demonstrated that, with a moderate laser intensity ($\sim 10^{14}$ W/cm^2), an isolated attosecond pulse of ~ 220 as can be generated with the two-color laser pulse consisting of a 35-fs/800-nm pulse and a 46-fs/1150-nm pulse. Chen *et al.*[22] generated isolated sub-50-as pulses using a multicycle 800-nm laser pulse in combination with a controlling 1600-nm laser pulse. Tang *et al.*[23] proposed a scheme to generate isolated attosecond pulses by high-peak-power multicycle laser fields, and they also showed that an isolated 100-as pulse can be generated with a duration of 50 fs. Kim *et al.*[24] systematically investigated the effect of the mixing of pulsed two color fields on the generation of an isolated attosecond pulse, and also demonstrated that a sub-100-attosecond pulse can be produced using an 11-fs 800-nm laser pulse with a proper mixing of a 1840-nm pulse.

To generate an isolated attosecond pulse with a shorter duration, the continuous spectrum used for synthesizing a single attosecond pulse should be broadened. Recent research results show that, by introducing a chirp to the laser pulse, the HHG cutoff can be enormously enlarged. The underlying physics behind this phenomenon is that the chirp can effectively increase the optical cycle of the driving laser field, after the laser reverses its direction, the quasifreely electron experiences a longest time acceleration when returning to the parent ion and obtains much higher kinetic energy from the driving laser field; as a result, the cutoff position of HHG is extended significantly. Moreover, this approach also has the potential to select a short or long quantum path, which leads to the production of isolated short attosecond pulses, such as a 108-as pulse via an intense few-cycle chirped pulse,[25] a 10-as pulse with phase compensation using a chirped few-cycle laser and a static electric field,[26] a 37-as (57-as) pulse by an intense few-cycle chirped laser and a half cycle pulse (an ultraviolet attosecond pulse),[27,28] a 59-as pulse by a multicycle chirped pulse combined with a chirp-free pulse,[29] a 31-as (5-as) pulse without (with) phase compensation using a two-color laser pulse with the combined chirps,[30] a 102-as pulse with a multicycle chirped and chirp-free two-color field,[31] a sub-24-as pulse with phase compensation using multi-cycle chirped polarization gating pulses,[32] and an intense isolated sub-40-as pulse generation in pre-excited He-ionic medium with the use of a same-frequency laser field synthesis.[33] In our previous work,[34] by combining a 9-fs/800-nm fundamental chirped pulse and a 9-fs/1600-nm controlling chirped pulse, we realized a 1342-eV supercontinuum with a short path contribution and also obtained an isolated 28-as pulse with a bandwidth of 155 eV.

HHG in the presence of a static electric field has been extensively investigated.[35–42] It has been shown that a static electric field is a very useful means to control the high harmonic emission rate,[35] the maximum harmonic photon energy,[36–39] and the polarization properties of harmonics.[40] Zhao *et al.*[41] reported HHG from a combination of a single-color 800-nm pulse and a static electric field and gave the expression for the continuum bandwidth, which is a function of the relative strength ratio and the few-cycle pulse's intensity and wavelength through the classical perspective. Our recent simulation calculation showed that a static electric field can not only modulate the quantum paths of the HHG, but also increase the ionization yield of electrons contributing to the continuous spectrum; as a result, the extension and enhancement of the HHG spectrum are achieved synchronously, which results in the production of an intense isolated 26-as pulse.[42] In this paper, the motivation of our simulation lies in the following considerations: first, though isolated attosecond pulse generations from the single chirped pulse,[25,43] the single chirped pulse or two-color laser in combination with a static electric field,[26,44] and two-color chirped pulse[28–34] have been investigated, few studies have been reported for the combination of the multicycle two-color chirped pulse and a static electric field; second, one of the current theoretical methods for producing single ultrashort attosecond pulses is by using the phase compensation for an achievable supercontinuum spectrum, which is not easy to achieve in an experiment; third, we intend to generate a single attosecond pulse with a duration below one atomic unit of time by straightforwardly filtering a large range of harmonics. Due to these ideas, in this paper we further investigate the HHG and isolated attosecond pulse generation of a model Ne atom in a multicycle two-color chirped laser and a static electric field. The calculated results show that with the combination of the multicycle two-color chirped laser and static electric field, not only the harmonic cutoff is significantly extended, but also the single short quantum path is selected to contribute to the HHG emission. By superposing some properly selected harmonics from continuum on HHG spectrum, an isolated 23-as pulse is directly generated without the phase compensation. Moreover, the simulation calculations also show isolated sub-30 pulses can be generated in a wide intensity range. These results are analyzed based on the three-step model and the time-frequency analysis of HHG.

2. Theoretical model and method

The HHG spectrum and attosecond pulse generation can be studied by numerically solving the one-dimensional time-dependent Schrödinger equation with the splitting operator method, which is based on the single-active-electron approximation and has been widely employed for HHG simulation. The harmonic spectrum is obtained by Fourier-transforming the time-dependent dipole acceleration from the Ehrenfest theorem.[45] The temporal profiles of the attosecond pulses

can be generated by simply performing the inverse Fourier transformations of the XUV supercontinua in different spectral regions. In our calculation, we use the soft-core potential model $V(x) = -1/\sqrt{x^2+a^2}$ and choose the softening parameter $a = 0.817$ to match the ionization energy of 21.56 eV for the ground state of a real Ne atom. The driving pulse is composed of a two-color chirped field (fundamental chirped pulse: 10-fs, 800 nm; subharmonic chirp-free pulse: 10-fs, 1760 nm) and a static field. The intensities of the fundamental chirped, subharmonic, and static fields are 4.0×10^{14}, 2.8×10^{13}, and 4.0×10^{13} W/cm^2, respectively. The electric field of the driving pulse can expressed as

$$E(t) = f(t)\{E_1\cos[\omega_1 t+\delta(t)]+E_2\cos(\omega_2 t)\}+E_3, \quad (1)$$

where $f(t) = \exp[-4\ln(2)(t/\tau)^2]$ is the envelope function, and $\tau = 10$ fs is the pulse duration of the laser field. E_i and ω_i $(i = 1,2)$ are the electric field amplitudes and the frequencies of the 800-nm fundamental chirped pulse and 1760-nm subharmonic chirp-free pulse, respectively. E_3 is the peak amplitude of the static electric field. $\delta(t) = -\beta\tanh[(t-t_0)/\tau_0]$ is the time profile of the CEP of the chirped pulse. The chirp form is controlled by adjusting the three parameters β, t_0, and τ_0. Due to the recent advancement of comb laser technology,[25,46,47] it is highly likely that such a time-varying CEP can be achieved in the near future. In the present work, β, τ_0, and t_0 are chosen to be 6.25, 200 a.u., and 0, respectively.

3. Results and discussion

In order to verify our scheme, we first investigate the HHG process according to the semiclassical three-step model, which presents a clear physical picture. Figure 1(a) describes the electric field of the two-color chirped field. Figure 1(b) presents the corresponding dependence of the harmonic order on the ionization and the recombination times. For the two-color chirped case, the electrons are mainly ionized near the peaks of the electric field and form three main peaks marked as A_1, B_1, and C_1 on the returning energy map, which are caused by the three time recollisions (marked as R_1, R_2, and R_3) in the profile of the laser field in Fig. 1(a). The maximum order harmonics of the peaks A_1, B_1, and C_1 are 183, 378, and 175, respectively, corresponding to harmonic energies I_p+284 eV, I_p+586 eV, and I_p+271 eV. In addition, the energy difference between A_1 and B_1 is 302 eV, which leads to the formation of the supercontinuum with a 302-eV bandwidth. It can be seen from Fig. 1(b) that for the harmonics with energies beyond I_p+284 eV each order harmonic is generated only through two electron trajectories (so-called long and short trajectories). The trajectory with an earlier ionization time but a later emission time is called the long trajectory, and the other trajectory with a later ionization time but an earlier emission time is called the short trajectory. The interference of the long and the short trajectories will lead to a modulated structure of the supercontinuum. As the harmonic order increases, the emission time for the short trajectory increases,

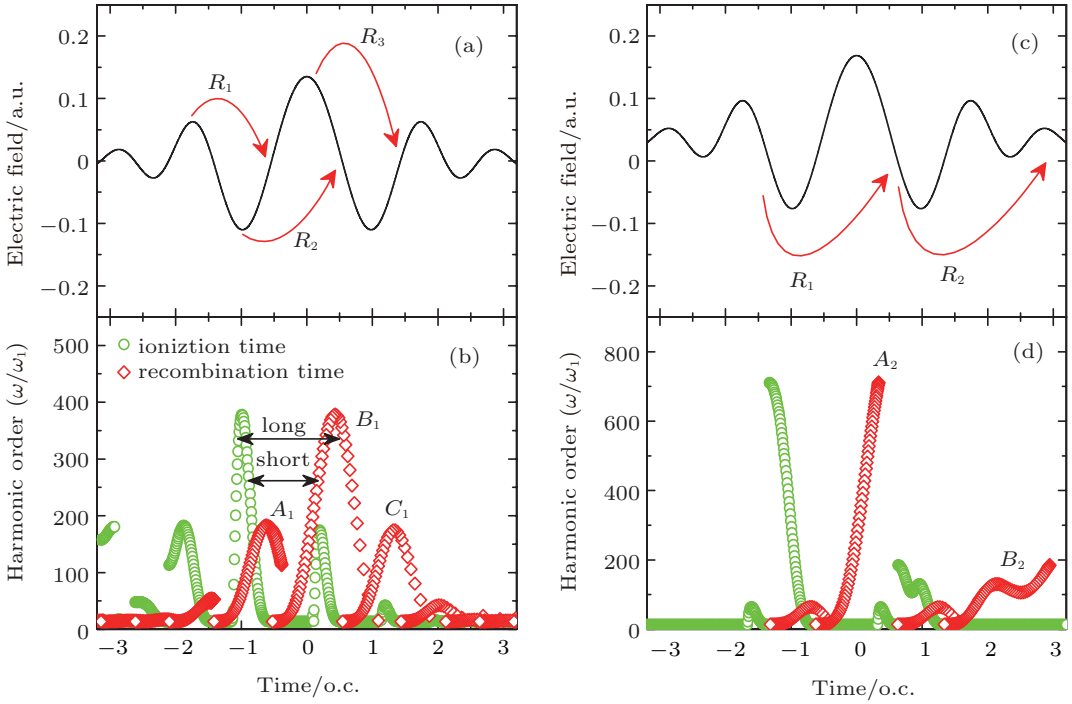


Fig. 1. (color online) Results of the two-color chirped field are displayed in the left-hand column and the combined results are displayed in the right-hand column: (a) and (c) driving laser field, (b) and (d) classical ionization and returning energy maps. The intensities of the fundamental chirped, subharmonic chirp-free, and static electric fields are 4.0×10^{14}, 2.8×10^{13}, and 4.0×10^{13} W/cm^2, respectively. The o.c. represents the optical cycle of the 800-nm free-chirp pulse throughout this paper.

and that for the long trajectory decreases, and at last these two emission times become equal. This result indicates that the harmonics in the second plateau are not synchronically emitted, and the harmonics in the cutoff are synchronized. Therefore, the superposition of several plateau harmonics will give out two bursts in each optical cycle of the fundamental pulse. The above results also imply that a single quantum contribution and an isolated attosecond pulse generation cannot be achieved by the two-color chirped field.

By adding a static electric field to the two-color chirped field, i.e., in the combined field case, the electron trajectories for HHG in the two-color chirped field can be significantly modulated. The sketch of the electron dynamics are shown in Figs. 1(c) and 1(d). Figure 1(c) presents the electric field of the two-color chirped field in combination with a static electric field. As shown in this figure, the electron is no longer ionized near the peak of the driving field, instead it is ionized from -1.33 o.c. to -0.66 o.c. and from 0.61 o.c. to 1.28 o.c. and forms two dominant returns (marked as R_1 and R_2). It is clear that the positive amplitude of the main peak is enhanced, and in contrast, the negative amplitudes of the two adjacent half-cycles are weakened; therefore, the electron ionized at -1.33 o.c. gains a much higher energy by the process R_1, which is responsible for the extension of the harmonic cutoff energy. To substantiate such a fact, we present the dependence of the harmonic order on the ionization and the recombination times, and the result is shown in Fig. 1(d). There are two major peaks marked as A_2 and B_2 on the returning energy map, which are caused by the two major time recollisions. The maximum order harmonic of A_2 reaches 711, whereas that of B_2 reaches 185. Compared with the two-color chirped case, since the highest order of the harmonics is much more higher, the spectral cutoff for the case is greatly extended. In addition, the energy difference between A_2 and B_2 is 816 eV, thus a broad supercontinuum covering a 816-eV bandwidth is generated and is superior to that for the two-color chirped case. From Fig. 2(d), we note that, in the range of peak A_2, only the short path is selected to contribute to the harmonic generation. This implies that the harmonics for the peak A_2 are almost locked in phase and emit simultaneously, because the phase-locked harmonics cover an extremely broad bandwidth, which is beneficial to generate an ultrashort isolated attosecond pulse.

To confirm the above results attained from the semiclassical model, we investigate the harmonic spectrum and the attosecond pulse generation using the full quantum calculation. In our calculations, the laser parameters are the same as those in Fig. 1. In Fig. 2, we show the harmonic spectra of the Ne atom in single chirped field, in the two-color chirped field and in the combined field, respectively. Since the low order harmonic spectra have the overlap in the cases of the three optical fields, so the spectral intensities of the two-color chirped and

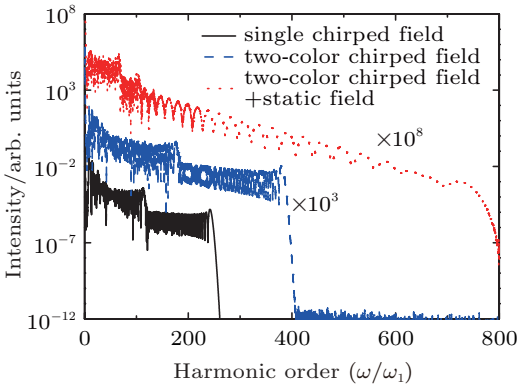


Fig. 2. (color online) Harmonic spectra of the Ne atom in the single chirped field (solid black curve), in the two-color chirped field (dashed blue curve), and in the combined field (dotted red curve). For the purpose of clarity, the harmonic intensities of the two-color chirped and combined fields are multiplied by factors of 10^3 and 10^8, respectively. Laser parameters are the same as those in Fig. 1.

combined field are multiplied by factors of 10^3 and 10^8 for the purpose of clarity. For the single chirped field case, the spectral cutoff is only at the 242nd-order harmonic, and the harmonics higher than the 112nd order are continuous, corresponding to a supercontinuum with a 202-eV bandwidth. For the two-color chirped case, the harmonic spectrum shown by the dashed blue curve in Fig. 2 presents a double-plateau structure with two cutoffs of the 175th order and the 378th order. The harmonics from the 183rd to the cutoff become continuous, forming a 302-eV supercontinuum (i.e., the whole second plateau). By comparison with the harmonic spectrum using the single chirped field, the width of the HHG plateau is significantly extended by 65 harmonics in the two-color chirped field. Thereby, the leading role of the subharmonic field of the two-color chirped field is the extension of the HHG plateau for the Ne atom. In addition, one can see that the supercontinuum for the above two cases shows a strongly modulated structure, which is owing to the interference between the long and short trajectories. It is well known that the strongly modulated supercontinuum with two quantum path contributions is not beneficial to generate an isolated attosecond pulse. With the addition of the static field, the electron trajectory is modified, and then only the short trajectory corresponding to the highest energy is selected to effectively contribute to the HHG generation. Thus the interference will be weak and the harmonic spectrum shows a fascinating structure, namely it becomes more regular and smooth. The harmonic spectrum in the presence of the static field is shown by the dotted red curve in Fig. 2. Clearly, the spectral cutoff for the case is significantly extended to the 728th-order harmonic, and the harmonics from the 185th order to the cutoff region are regular and continuous, corresponding to a supercontinuum with a 833-eV bandwidth. Compared with the case of using the two-color chirped field, the bandwidth of the supercontinuum in the presence of the static field becomes much broader. Further, the modulation

in the supercontinuum is largely removed, implying that one single quantum path is selected.

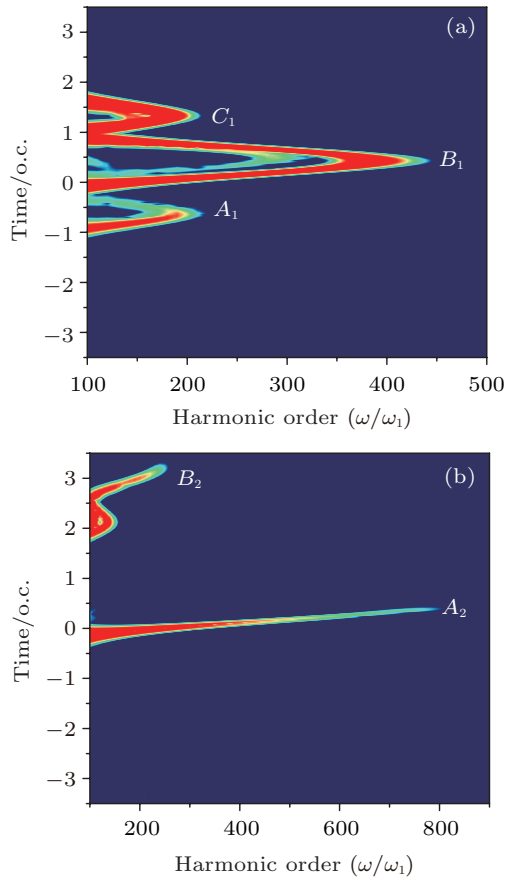


Fig. 3. (color online) Time-frequency distributions of the HHG spectra: (a) the two-color chirped field, (b) the combined field. Laser parameters are the same as those in Fig. 1.

A deeper insight is obtained by investigating the emission times of the harmonics in terms of the time-frequency analysis method.[48] The result is shown in Fig. 3. For comparison, the time-frequency distribution of the HHG spectrum in the two-color chirped case is also shown in Fig. 3(a). As shown in this figure, there are three main peaks labelled by A_1, B_1, and C_1 contributing to the harmonic generation. The maximum harmonic orders of A_1, B_1, and C_1 are approximately at the 183rd, 378th, and 175th orders, respectively. Among these three peaks, the intensity of C_1 is stronger than the intensities of A_1 and B_1, in other words, the harmonic yields of C_1 are much higher than those of A_1 and B_1, which is the reason for the two-plateau structure. Furthermore, the harmonics above the 185th order are only contributed by B_1, forming a 302-eV supercontinuum. However, the supercontinuum origins from the contributions of the two quantum paths (the negative-slope branch: the long quantum path; the positive-slope branch: the short quantum path), the interference between them brings about an obviously modulated structure in the supercontinuum, as shown by the dashed blue curve in Fig. 2. Figure 3(b) is the time-frequency distribution of HHG in the combined field. As seen from this figure, there are two major peaks labelled by A_2 and B_2 in the time-frequency distribution. The maximal harmonic orders of peaks A_2 and B_2 are about 722 and 185, respectively. The harmonics above the 185th order only originate from the contribution of A_2, forming an ultrabroad supercontinuum with a bandwidth of 833 eV. For the harmonics below the 185th order, the interference between the peaks A_2 and B_2 leads to an irregular spectral structure, which is shown by the dotted red curve in Fig. 2. Additionally, there is only one short quantum path contributing to the supercontinuum, i.e., the short-path harmonic is effectively selected, which is responsible for a broadband smooth supercontinuum and at the same time indicates that the selection of the single short path is achieved after the use of the static field. The above results are basically consistent with those with the classical approaches.

Next, we consider the attosecond pulse generation in the combined field. For comparison, the generated attosecond pulse in the two-color chirped field is presented in Fig. 4(a). As shown in this figure, by superposing the harmonics from the 240th to the 285th order, two main attosecond pulses with durations of 60-as and 58-as are generated, respectively. This is because there are two quantum paths with different emission times contributing to the same harmonic (as seen in Fig. 3(a)), and as the harmonics in the supercontinuum region are not emitted in phase, the superposition of several harmonics will result in an attosecond pulse train containing two radiation pulses rather than an isolated attosecond pulse. As shown in Fig. 4(a), the strong 60-as pulse originates from the short path, the weak 58-as pulse originates from the long one. Such a chain of attosecond pulses are very difficult to use in the pump-probe experiment or the measurement of ultrafast dynamic processes. Figures 4(b)–4(d) show the temporal profile of the attosecond pulse in the combined field. We first superpose the harmonics from the 185th to the 741st order, i.e., the entire supercontinuum region, and an isolated 25-as pulse with accompanying satellite pulses is directly produced, as shown in Fig. 4(b). The intensity ratio of the strongest satellite pulse to the main pulse is approximately 53%. In order to obtain an isolated attosecond pulse with a relatively high signal-to-noise ratio, we only select a section of the harmonics from the supercontinuum region. As shown in Fig. 4(c), by superposing the harmonics from the 310th to the 420th order, an isolated 23-as pulse with several weak satellite pulses is directly obtained without any phase compensation. In the situation, however, the intensity of the strongest satellite pulse only occupies 0.36 of the main pulse, so the signal-to-noise ratio of the single attosecond pulse is further improved. The isolated 23-as pulse contains only 3.14 optical cycles of the central wavelength of 2.19 nm. Such a short isolated attosecond pulse will enable the detection and the control of the electronic dynamics inside atoms and molecules. It should be noted that our calculations

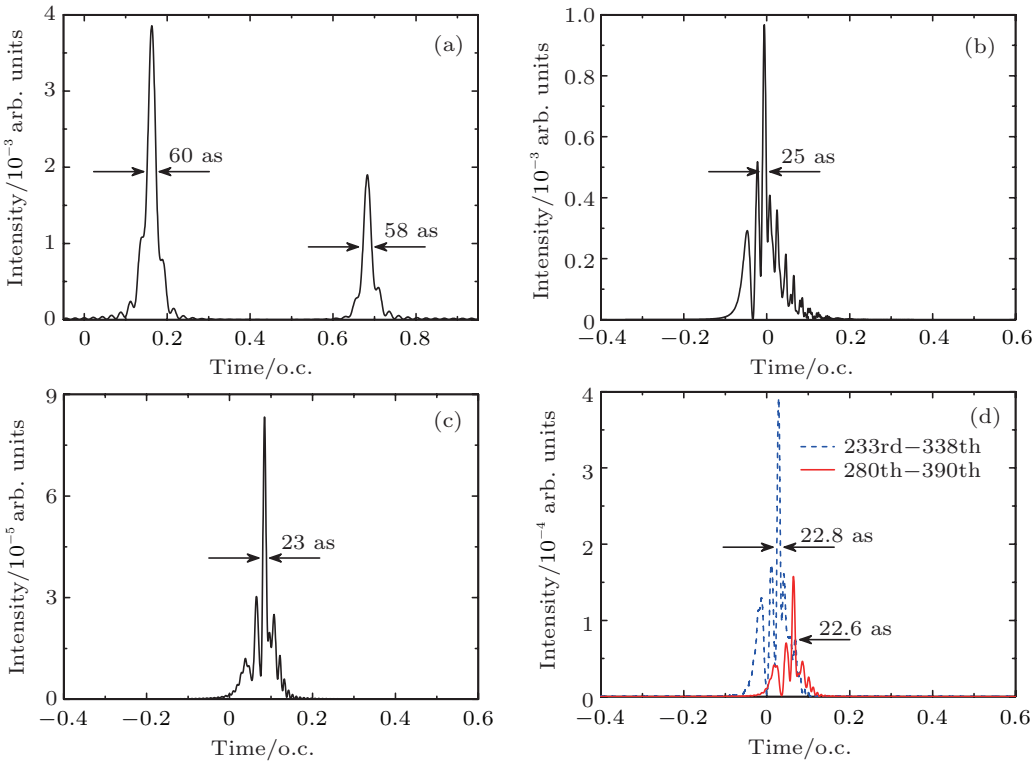


Fig. 4. (color online) Temporal profile of the attosecond pulse by superposing some harmonics in the supercontinuum: (a) the two-color chirped field, (b)–(d) the combined field. Laser parameters are the same as those in Fig. 1.

show that the single attosecond pulse presented in Fig. 4(c) can be obtained by superposing some well-chosen continuous harmonics in the supercontinuum, as shown in Fig. 4(d), which provides a convenient approach to obtain an isolated ultrashort attosecond light pulse with stable pulse duration in an experiment.

In this work, by applying the static field to the two-color chirped field, we further extend both the harmonic cutoff and the supercontinuum width. But we want to know what the effect of the static field is. For the purpose of clarify, we investigate the harmonic spectra in the combined field with four different intensities of the static field (I_3). Other parameters are the same as those in Fig. 1. Figure 5(a) presents our calculated results. As shown in this figure, the harmonic spectrum is sensitive to the variation of the intensity of the static field. If the static field strength is relatively weak, the harmonic spectrum presents a large modulation structure, but it has a short cutoff, which also decreases the width of the supercontinuum. Contrarily, if the static field strength is relatively strong, the spectral modulation becomes small, and the harmonic spectrum becomes smooth, but the spectral cutoff becomes short, resulting in the reduction of the supercontinuum width. To further explore the detail between the harmonic cutoff or the supercontinuum and the static field strength, we investigate the HHG processes in the combined field with different static field strengths by the semiclassical three-step model. Figure 5(b) shows the dependences of the 1st and the 2nd cutoffs of the HHG on the static field strength. As the static field strength changes from 1.5×10^{13} W/cm^2 to 7.0×10^{13} W/cm^2, the second cutoff of the spectrum increases from 1.5×10^{13} W/cm^2 to 3.6×10^{13} W/cm^2, reaches a maximum at $I_3 = 3.6\times10^{13}$ W/cm^2, and then decreases to the 601st order at $I_3 = 7.0\times10^{13}$ W/cm^2, whereas the first cutoff of the spectrum has no significant change (from the 150th to the 196th order). In the light of the definition of a continuum spectrum in Ref. [49], namely, the frequency difference between the highest and the second-highest cutoffs, in our method, the supercontinuum is the broadest for the case of $I_3 = 4.0\times10^{13}$ W/cm^2. In this case, a supercontinuum covering an 816-eV bandwidth is generated. Though the spectral cutoff is the highest at $I_3 = 3.6\times10^{13}$ W/cm^2, the width of the supercontinuum (i.e., 805 eV) for the case is lower than that at $I_3 = 4.0\times10^{13}$ W/cm^2. Thus we show that the optimal intensity of the static electric field is $I_3 = 4.0\times10^{13}$ W/cm^2. In our method, we also consider how long Ne can survive in the static field alone. From our calculation, the ionization probability of Ne is lower than 0.12 when the duration of the static field is not longer than 1 ps. Moreover, we also investigate the influence of the static field strength on the harmonic efficiency. As the intensity of the static field varies from 3.0×10^{13} W/cm^2 to 6.0×10^{13} W/cm^2, the harmonic spectrum has no distinct changes in HHG efficiency. As the intensity of the static field is lower than 3.0×10^{13} W/cm^2, the spectral efficiency is relatively high compared with that in the range of the static field

strength mentioned above, but the harmonic cutoff and the supercontinuum become short. As the intensity of the static field is higher than 6.0×10^{13} W/cm^2, the harmonic spectrum has a low conversion efficiency and narrow supercontinuum width. All in all, the harmonic efficiency tends to decrease for the relatively high static field strength under the present laser-matter condition. Therefore, in practical experiments with our scheme, a static field strength should be kept in the range from 3.0×10^{13} W/cm^2 to 6.0×10^{13} W/cm^2, which will help to obtain the broadband supercontinuum with a relatively high efficiency and less modulated structure.

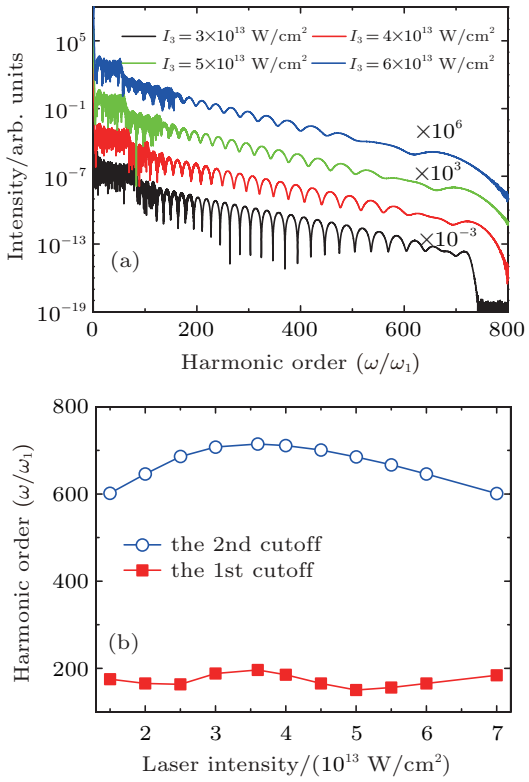


Fig. 5. (color online) (a) Harmonic spectra with four different intensities of the static electric field. (b) Dependences of the 1st and the 2nd cutoffs of the HHG on the intensity of the static electric field. Other parameters are the same as those in Fig. 1.

In Fig. 6, we investigate the influences of the wavelength (λ_2) and intensity (I_2) of the subharmonic chirp-free pulse on the harmonic spectrum. The other parameters are the same as those in Fig. 1. Figure 6(a) presents the harmonic spectra with six different wavelengths of the subharmonic chirp-free pulse. As shown in this figure, the harmonic spectrum is sensitive to the variation of the wavelength of the subharmonic chirp-free pulse. As the wavelength varies from 1200 nm to 2800 nm, the spectral cutoff increases from 1200 nm to 1760 nm, reaches the maximum cutoff of the 728th order at $\lambda_2 = 1760$ nm, and then decreases to the 533rd order at $\lambda_2 = 2800$ nm. To further explore the detail between the harmonic cutoff and the wavelength of the subharmonic pulse, we plot out the curve of the spectral cutoff with respect to the wavelength of the subharmonic pulse by the three-step model in Fig. 6(b). From this figure, for the cases of $\lambda_2 < 1690$ nm, the spectral cutoff increases with increasing the wavelength. For the cases of $\lambda_2 > 1830$ nm, the spectral cutoff decreases with increasing the wavelength. However, when the wavelength varies from 1690 nm to 1830 nm, the harmonic cutoff is not much changed (the harmonic cutoff is about the 710th order, as shown by the magenta dotted line in Fig. 6(b)). Therefore, in our method, the wavelength of the subharmonic pulse can be chosen in a wide interval, which makes one facilitate the experimental implement for the broadband supercontinuum generation. On a separate note, the wavelength of the subharmonic pulse in our

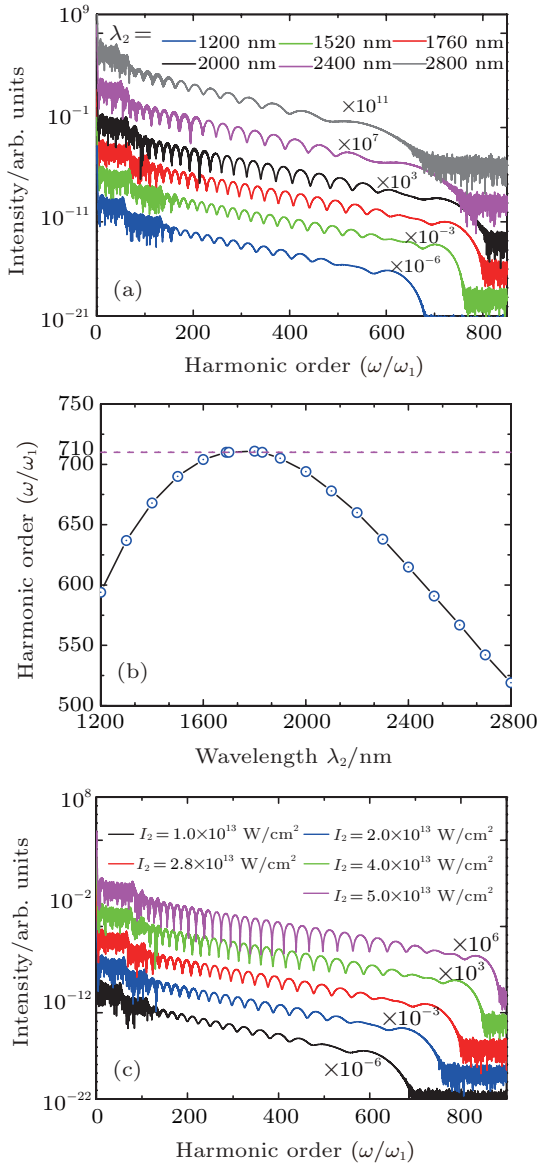


Fig. 6. (color online) (a) Harmonic spectra with six different wavelengths of the subharmonic chirp-free pulse. (b) The curve of the spectral cutoff with respect to the wavelength of the subharmonic pulse. (c) Harmonic spectra with five different intensities of the 1760-nm subharmonic chirp-free pulse. Other parameters are the same as those in Fig. 1.

simulation is chosen to be 1760 nm for convenience in discussion and for clarity. Next, we investigate the influence of the intensity of the 1760-nm subharmonic pulse on the harmonic spectrum. From our calculation, we find that increasing the intensity of the subharmonic pulse will result in the extension of the harmonic cutoff and the widening of the supcontinuum. Figure 6(c) presents the harmonic spectra with five different intensities of the 1760-nm pulse. Clearly, with the increase of the intensity of the subharmonic pulse, the first cutoff of the spectrum has no significant change, whereas the second one of the spectrum is markedly enlarged; thus the frequency difference between the first and the second cutoffs is enhanced, which also leads to the extension of the supercontinuum spectrum. This unique property can be used for producing a broadband supercontinuum, which helps to experimentally generate an ultrashort isolated attosecond pulse. In addition, we also find from our simulation that the efficiency of the supercontinuum is improved actually by increasing the intensity of the subharmonic pulse to some extent. From this point of view, to increase the intensity of the subharmonic pulse is an efficient method for enhancing the harmonic efficiency. The reason is as follows: in our method, the continuous harmonics originate from electrons ionized in the half cycle with the second-highest electric field peak (i.e., electrons ionized in the time range from -1.33 o.c. to -0.66 o.c.), when the intensity of the subharmonic pulse increases, the second-highest electric field peak of the combined field is enhanced, the ionization yields of the corresponding electrons are increased, as a result, the conversion efficiency of the continuous harmonics is improved. Note that the plateau harmonics exhibit a deep modulation structure and only the cutoff harmonics are continuous for the case of the laser intensity beyond 5.0×10^{13} W/cm^2, which is not good for the generation of an intense isolated attosecond pulse. For the cases of other wavelength values, we find that similar results can be obtained in terms of the above discussion.

In order to check how sensitive the harmonic spectrum is to the intensity of the fundamental chirped pulse, Fig. 7 shows the harmonic spectra generated in the combined field with four different intensities of the fundamental chirped pulse. According to our calculations, the same is true if the intensity of the fundamental chirped pulse is increased, as shown in Fig. 7. Just the spectral cutoff and the bandwidth of the supercontinuum are greatly extended in comparison with that in Fig. 6(c). Furthermore, with the increase of the intensity of the fundamental chirped pulse, the low-energy part of the harmonic spectrum shows a more pronounced modulation structure. The characteristic behavior can be further seen by the green curve in Fig. 7 with $I_1 = 6.0 \times 10^{14}$ W/cm^2, where the modulation structure in the low-energy part is so obvious that it cannot generate a single short attosecond pulse generation. However, the high-energy one of the spectrum, i.e., the harmonics near the cutoff, is still smooth, which can support us in generating an isolated ultrashort attosecond pulse by filtering some properly selected harmonics. Additionally, we find that the increases of the intensity of the fundamental chirped pulse will result in the uplift of all the harmonic spectra, implying an enhancement of the harmonic efficiency. This reason is similar to the one we analyzed in Fig. 6. But it might also be noted that an extremely high driving field will lead to the ionization saturation of the target atom and limit the harmonic yields. However, under the present laser-matter condition, we calculate the ground state population and find that the depletion of the ground state does not appear when the time evolution of the pulse ends. Consequently, in our method, increasing the intensity of the fundamental chirped pulse may be a very productive line of enhancing the harmonic efficiency.

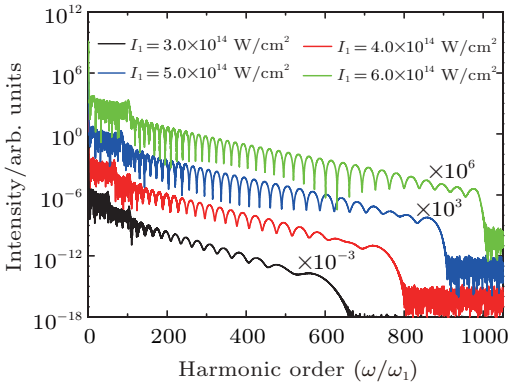


Fig. 7. (color online) Harmonic spectra with four different intensities of the 800-nm fundamental chirped pulse. Other parameters are the same as those in Fig. 1.

Finally, we analyze the influence of the fluctuations of the laser intensities on the broad bandwidth isolated sub-30-as pulse. From our simulation, when the intensity of the fundamental chirped pulse changes from 3.1×10^{14} W/cm^2 to 5.5×10^{14} W/cm^2, we can obtain a broadband isolated sub-30-as pulse with the satellite pulse less than 50% of the main pulse intensity by superposing properly continuous harmonics, as shown in Fig. 8(a). The same is true even if the intensity of the subharmonic chirp-free pulse changes from 1.2×10^{13} W/cm^2 to 5.0×10^{13} W/cm^2, which is shown in Fig. 8(b). For the static electric field, when its intensity changes from 2.2×10^{13} W/cm^2 to 5.8×10^{13} W/cm^2, an isolated broadband sub-30-as pulses can be obtained, and the intensity ratio of the satellite pulse to the main pulse is below 50%, as shown in Fig. 8(c). The above results show that isolated broadband sub-30-as pulses can be generated in a wide

range of laser intensity, which is particularly favorable for producing an isolated ultrashort attosecond light pulse with a stable pulse duration in an experiment.

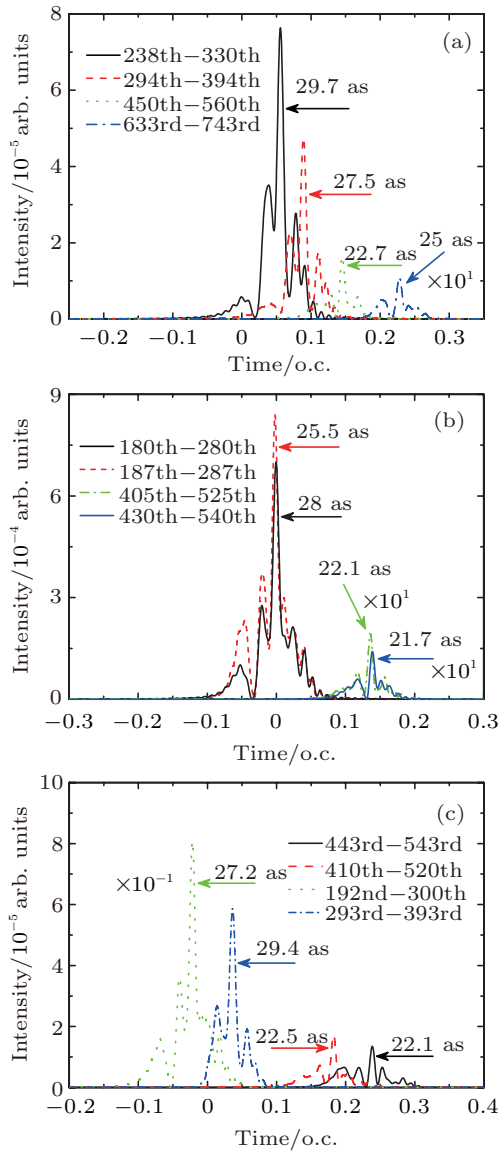


Fig. 8. (color online) Temporal profiles of isolated attosecond pulses generated from the continuous harmonics in the combined field with different laser intensities: (a) from the 238th to the 330th order for $I_1 = 3.1 \times 10^{14}$ W/cm^2 (solid black curve); from the 294th to the 394th order for $I_1 = 3.5 \times 10^{14}$ W/cm^2 (dashed red curve); from the 450th to the 560th order for $I_1 = 5.0 \times 10^{14}$ W/cm^2 (dotted green curve); from the 633rd to the 743rd order for $I_1 = 5.5 \times 10^{14}$ W/cm^2 (dashed–dot blue curve). (b) The same as panel (a) but for four different intensities of the subharmonic chirp-free pulse of 1.2×10^{13}, 2.0×10^{13}, 4.0×10^{13}, and 5.0×10^{13} W/cm^2, respectively. (c) The same as panel (a) but for four different intensities of the static electric field of 2.2×10^{13}, 3.0×10^{13}, 5.0×10^{13}, and 5.8×10^{13} W/cm^2, respectively. Other parameters are the same as those in Fig. 1.

4. Conclusions

In conclusion, we have theoretically presented an efficient method for generating an isolated ultrashort attosecond pulse in a multicycle two-color chirped laser in combination with a static electric field. It is shown that the quantum path of the HHG by the two-color chirped field can be effectively controlled in the presence of the static field. As a result, not only is the harmonic cutoff significantly extended, but also the supercontinuum width is greatly enlarged. In addition, since the supercontinuum spectrum covers an extremely broad bandwidth and originates from the contribution of the single quantum path, an ultrashort isolated 23-as pulse with a 170.6-eV bandwidth is straightforwardly obtained without any phase compensation. Further, we also investigated the influence of the fluctuations of the laser intensities on the supercontinuum and isolated attosecond pulses. The calculated results show that a supercontinuum with a broad bandwidth and isolated attosecond pulses with durations of less than 30-as can be produced in a wide intensity range. For the 800-nm fundamental pulse, its intensity should be kept in the range of 3.1×10^{14} W/cm^2 $\sim$ 5.5×10^{14} W/cm^2. For the 1760-nm subharmonic laser pulse, its intensity should be limited in the range of 1.2×10^{13} W/cm^2 $\sim$ 5.0×10^{13} W/cm^2 (note that the intensity range is suitable for the subharmonic pulse with the wavelength of 1690 nm $\sim$ 1830 nm). For the static field, its intensity should be controlled in the range of 3.0×10^{13} W/cm^2 $\sim$ 5.8×10^{13} W/cm^2. These properties are very beneficial to the experimental implement for the generation of the isolated ultrashort attosecond pulses with stable pulse durations. Finally, we would like to point out the feasibility of the scheme. Currently, a 10-fs, 800-nm laser pulse is available in a good few laboratories, and a 10-fs subharmonic pulse with the wavelength of 1690 nm $\sim$ 1830 nm pulse can be generated by optical parametric amplifier (OPA) from an 800-nm laser pulse. The static field strength used in this paper is extremely high so that it is not experimentally possible nowadays. However, it has been shown that a low-frequency laser field (such as CO_2 lasers)[26,35,40,50] or a strong terahertz field[38,51] can be used instead of the high static field. Our simulation calculations also indicate that, by adding a THz field with a wavelength range of 50 μm $\sim$ 100 μm to the two-color chirped field, similar results are obtained. From our calculations, we find that such an effective controlling scheme can also use a combined field with the duration of 30 fs, which makes our scheme more achievable in experiments. In a word, the advantages of the scheme proposed here lies in generating a broadband XUV supercontinuum with a single quantum path contribution, which is beneficial for producing an isolated ultrashort attosecond pulse.

References

[1] McFarland B K, Farrell J P, Bucksbaum P H and M Guhr M 2008 *Science* **322** 1232

[2] Shafir D, Mairesse Y, Villeneuve D M, Corkum P B and Dudovich N 2009 *Nat. Phys.* **5** 412
[3] Kanai T, Minemoto S and Sakai H 2005 *Nature* **435** 470
[4] Corkum P B 1993 *Phys. Rev. Lett.* **71** 1994
[5] Hentschel M, Kienberger R, Spielmann C, Reider G A, Milosevic N, Brabec T, Corkum P B, Heinzmann U, Drescher M and Krausz F 2001 *Nature* **414** 509
[6] Kienberger R, Goulielmakis E, Uiberacker M, Baltuska A, Yakovlev V, Bammer F, Scrinzi A, Westerwalbesloh T, Kleineberg U, Heinzmann U, Drescher M and Krausz F 2004 *Nature* **427** 817
[7] Goulielmakis E, Schultze M, Hofstetter M, Yakovlev V S, Gagnon J, Uiberacker M, Aquila A L, Gullikson E M, Attwood D T, Kienberger R, Krausz F and Kleineberg U 2008 *Science* **320** 1614
[8] Chang Z H 2005 *Phys. Rev. A* **71** 023813
[9] Sansone G, Benedetti E, Calegari F, Vozzi C, Avaldi L, Flammini R, Poletto L, Villoresi P, Altucci C, Velotta R, Stagira S, Silvestri S D and Nisoli M 2006 *Science* **314** 443
[10] Zhang Q B, Lu P X, Lan P F, Hong W Y and Yang Z Y 2008 *Opt. Express* **16** 9795
[11] Chang Z H 2007 *Phys. Rev. A* **76** 051403(R)
[12] Mashiko H, Gilbertson S, Li C, Khan S D, Shakya M M, Moon E and Chang Z H 2008 *Phys. Rev. Lett.* **100** 103906
[13] Feng X M, Gilberston S, Mashiko H, Wang H, Khan S D, Chini M, Wu Y, Zhao K and Chang Z H 2009 *Phys. Rev. Lett.* **103** 183901
[14] Zhao K, Zhang Q, Chini M, Wu Y, Wang X W and Chang Z H 2012 *Opt. Lett.* **37** 3891
[15] Yudin G L, Bandrauk A D and Corkum P B 2006 *Phys. Rev. Lett.* **96** 063002
[16] Mauritsson J, Johnsson P, Gustafsson E, L'Huillier A, Schafer K J and Gaarde M B 2006 *Phys. Rev. Lett.* **97** 013001
[17] Pfeifer T, Gallmann L, Abel M J, Neumark D M and Leone S R 2006 *Opt. Lett.* **31** 975
[18] Cao W, Lu P X, Lan P F, Wang X L and Yang G 2007 *Opt. Express* **15** 530
[19] Luo J H, Hong W Y, Zhang Q B, Liu K L and Lu P X 2012 *Opt. Express* **20** 9801
[20] Chen J G, Yang Y J and Chen Y 2011 *Acta Phys. Sin.* **60** 033202 (in Chinese)
[21] Zeng Z N, Leng Y X, Li R X and Xu Z Z 2008 *J. Phys. B: At. Mol. Opt. Phys.* **41** 215601
[22] Chen J G, Yang Y J, Zeng S L and Liang H Q 2011 *Phys. Rev. A* **83** 023401
[23] Tang S S and Chen X F 2012 *Phys. Rev. A* **85** 063816
[24] Kim B, Ahn J, Yu Y L, Cheng Y, Xu Z Z and Kim D E 2008 *Opt. Express* **16** 10331
[25] Carrera J J and Chu S I 2007 *Phys. Rev. A* **75** 033807
[26] Xiang Y, Niu Y P and Gong S Q 2009 *Phys. Rev. A* **79** 053419
[27] Li W, Wang G L and Zhou X X 2011 *Acta Phys. Sin.* **60** 123201 (in Chinese)
[28] Zhao S F, Zhou X X, Li P C and Chen Z J 2008 *Phys. Rev. A* **78** 063404
[29] Xu J J, Zeng B and Yu Y L 2010 *Phys. Rev. A* **82** 053822
[30] Feng L Q and Chu T S 2011 *Phys. Rev. A* **84** 053853
[31] Du H C and Hu B T 2011 *Phys. Rev. A* **84** 023817
[32] Zhang C J, Yao J P and Ni J L 2012 *Opt. Express* **20** 24642
[33] Mohebbi M and Batebi S 2012 *J. Electron. Spectrosc. Relat. Phenom.* **185** 578
[34] Zhang G T, Bai T T and Zhang M G 2012 *Commun. Theor. Phys.* **58** 557
[35] Odžak S and Miloševic D B 2005 *Phys. Rev. A* **72** 033407
[36] Wang B B, Li X F and Fu P M 1998 *J. Phys. B: At. Mol. Opt. Phys.* **31** 1961
[37] Wang B B, Li X F and Fu P M 1999 *Phys. Rev. A* **59** 2894
[38] Hong W Y, Lu P X, Cao W, Lan P F and Wang X L 2007 *J. Phys. B: At. Mol. Opt. Phys.* **40** 2321
[39] He H X, Guo Y H and He G Z 2012 *Chin. Phys. B* **21** 080202
[40] Borca1 B, Flege A V, Frolov M V, Manakov N L, Milošević D B and StaraceA F 2000 *Phys. Rev. Lett.* **85** 732
[41] Zhao G J, Guo X L, Shao T J and Xue K 2011 *New J. Phys.* **13** 093035
[42] Zhang G T, Bai T T and Zhang M G 2012 *Chin. Phys. B* **21** 054214
[43] Niu Y P, Xiang Y, Qi Y H and Gong S Q 2009 *Phys. Rev. A* **80** 063818
[44] Xia C L, Zhang G T, Wu J and Liu X S 2010 *Phys. Rev. A* **81** 043420
[45] Burnett K, Reed V C, Cooper J and Knight P L 1992 *Phys. Rev. A* **45** 3347
[46] Cundiff S T and Ye J 2003 *Rev. Mod. Phys.* **75** 325
[47] Udem T, Holzwarth R and Hänsch T W 2002 *Nature* **416** 233
[48] Antoine P, Piraux B and Maquet A 1995 *Phys. Rev. A* **51** R1750
[49] Zeng Z N, Cheng Y, Song X H, Li R X and Xu Z Z 2007 *Phys. Rev. Lett.* **98** 203901
[50] Wang B B, Cheng T W, Li X F and Fu P M 2005 *Phys. Rev. A* **72** 063412
[51] Hong W Y, Lu P X, Lan P F, Zhang Q B and Wang X B 2009 *Opt. Express* **17** 5139